Strain elastography with Ultrasound Computer Tomography: a simulation study based on biomechanical models

T. Hopp and N.V. Ruiter

Karlsruhe Institute of Technology (KIT), Germany
Institute for Data Processing and Electronics

ABSTRACT

Ultrasound computer tomography (USCT) is a promising modality for breast cancer diagnosis which images the reflectivity, sound speed and attenuation of tissue. Elastic properties of breast tissue, however, cannot directly be imaged although they have shown to be applicable as a discriminator between different tissue types. In this work we propose a novel approach combining USCT with the principles of strain elastography. So-called USCT-SE makes use of imaging the breast in two deformation states, estimating the deformation field based on reconstructed images and thereby allows localizing and distinguishing soft and hard masses. We use a biomechanical model of the breast to realistically simulate both deformation states of the breast. The analysis of the strain is performed by estimating the deformation field from the deformed to the undeformed image by a non-rigid registration. In two experiments the non-rigid registration is applied to ground truth sound speed images and simulated SAFT images. Results of the strain analysis show that for both cases soft and hard lesions can be distinguished visually in the elastograms. This paper provides a first approach to obtain mechanical information based on external mechanical excitation of breast tissue in a USCT system.

**Keywords:** Strain elastography, Ultrasound computer tomography, Biomechanical model

1. INTRODUCTION

Ultrasound computer tomography (USCT) is a promising modality for breast cancer diagnosis, which is approaching clinical applicability.[1–3] By acquiring signal data from all around the imaged object, it is able to derive reflectivity as well as transmission images. While reflectivity images qualitatively depict interfaces between tissues, transmission images provide a quantitative measure of the sound speed and acoustic attenuation in the object.

Elastic properties of breast tissue have shown to be applicable as a discriminator between different tissue types,[4] especially to distinguish between benign and malign masses.[5] For linear elastic material, the Young's modulus is coupled to the sound speed and density. For reconstruction of USCT images, the density contrast is yet mostly assumed to be constant. Hence the elastic properties can not directly be derived from the imaged properties. Approaches exist to estimate relative tissue stiffness by combining sound speed and attenuation images.[6]

Ultrasound elastography is an imaging technique, which estimates the elastic properties of tissue using mechanical excitation of the object. In quasi-static methods, the mechanical excitation is applied to the tissue by a constant stress, which results in a strain. This strain is approximated by estimating the deformation field between data acquired before and after the stress is applied.[7] Since the applied stress is usually unknown, this technique is able to derive only qualitative stiffness maps, in which hard and soft tissues can be distinguished relative to each other and/or relative to surrounding tissue. Such methods are therefore often be referred to as strain elastography or strain ratio elastography.[8] In contrast, dynamic methods mechanically excite the tissue by time-varying forces, e.g. by external vibration or using acoustic radiation force, and thereby induce shear waves within the tissue. By estimating the velocity of the shear wave traveling through the tissue and assuming a linear-elastic material, the Young's modulus can be calculated, resulting in a quantitative measure of the tissue stiffness.[7]
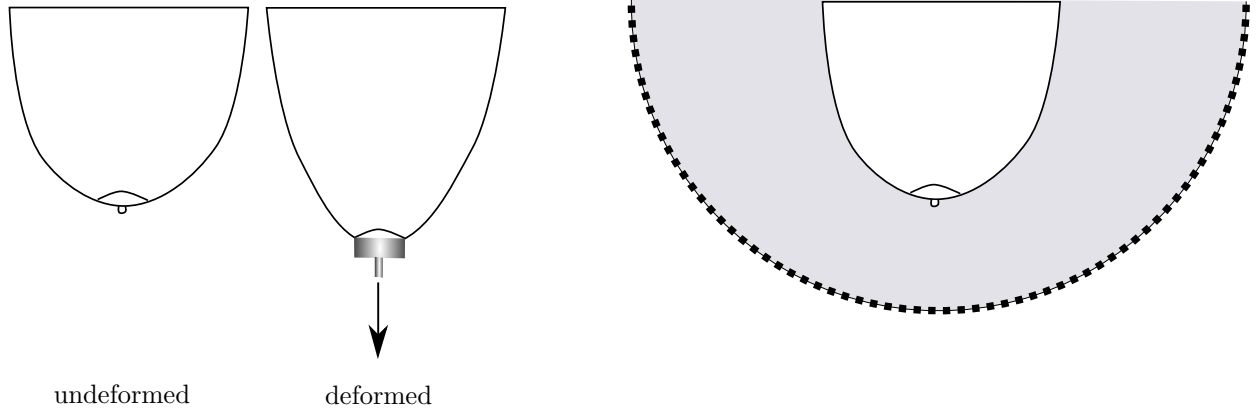
(a) Two deformation states of the breast: undeformed (left) and deformed (right) by pulling down the breast in the area around the mamilla by an according device.

(b) Illustration of the imaging principle: the breast is immersed into a water bath surrounded by e.g. a half sphere of transducers (black dots).

Figure 1: Illustration of the modeled imaging situation.

In this work we propose a novel approach combining USCT with the principles of elastography. Due to the potentially simple integration in existing USCT systems (see section 2), we decided to implement a strain-elastography (SE) approach. So-called USCT-SE makes use of imaging the breast in two deformation states, estimating the deformation field based on reconstructed images and thereby allows localizing and distinguishing soft and hard masses. A first simulation study is presented: we use a biomechanical model to simulate different deformation states of the breast (section 2.2) and simulate USCT images for both deformation states (section 2.3). Based on these images we estimate the strain using a non-rigid image registration (section 2.4).

2. METHODS

2.1 Basic idea

The basic idea of performing USCT-SE is to mechanically excite the breast tissue while acquiring the image data in a fixed setup of transducers. The mechanical excitation in the present paper is achieved during imaging in prone position by pulling the breast in an area around the mamilla downwards. Such a mechanical excitation may in practice be achieved without or with only small modifications of existing systems: For example, the SoftVue (Delphinus Medical Technologies)[*] and QTscan (QT ultrasound)[†] systems both use dedicated devices to pull down the breast in order to stabilize it during imaging in prone position.

In our proposed method, the breast is imaged in two deformation states: relaxed (referred to as "undeformed") and stretched (referred to as "deformed"), see Figure 1a). As in the conventional setup, we assume that reflectivity, sound speed and attenuation images can be reconstructed given the imaging aperture. In our evaluation we use a hemispherical setup (Figure 1b), similar to e.g. the distribution of transducer in the KIT 3D USCT device.[3] The raw data in such a USCT device is taken by sequentially emitting approximately spherical waves into a water bath surrounding the breast, while all other transducers in the aperture acquire the signal data. From the signal data, transmission and reflection images are reconstructed offline.

2.2 Simulation of deformation with biomechanical model

We use a biomechanical model of the breast based on our earlier work[9, 10] in order to simulate both deformation states of the breast. In this work we use a 2D model, which is constructed from a sagittal slice of a segmented MRI image. The segmentation distinguishes fatty and fibroglandular tissue, skin and muscle. Moreover we

---

[*]http://delphinusmt.com/

[†]https://www.qtultrasound.com

artificially inserted a tumor of diameter 1 cm. The model geometry is derived by meshing the pixels into a quadrilateral mesh. The mesh consisted of approx. 34,000 elements with an element size of 0.5 mm.

The tissues are modeled nearly incompressible with a Poisson's ratio of $\nu = 0.495$. Further tissue non-linearity is accounted for by a neo-hookean material model. Mechanical material parameters for fat, fibrograndular, skin, muscle and tumor tissue were derived from literature.[11, 12]

By restricting the upper-most nodes from moving, we model a rigid fixation of the breast at the body. The boundary conditions for the deformation simulation are defined by grouping surface nodes of the model in a radius of 1.5 cm around the mamilla and applying a displacement constraint downwards on them with an adjustable magnitude. In our experiments we applied a displacement of $10\,mm$. The computation is performed using the commercial FEM software ABAQUS using the dynamic FEM solver with quasi-static time stepping.

2.3 Simulation of USCT images

Based on the tissue labels in the segmented MRI we assigned the acoustic properties sound speed and attenuation as well as a density to every pixel with values taken from literature.[13] Thereby the images represent the tissue contrast in an idealized way, i.e. considering a perfect reconstruction. For our first experiment, we use the so derived sound speed image in its undeformed and deformed configuration. The deformed configuration was obtained by a linear interpolation of the deformation field. Each pixel position inside an element was expressed in barycentric coordinates with respect to the node positions after deformation. Afterward the barycentric coordinates were used as weighting factors for the displacements at the nodes in order to derive the according position in the undeformed element. Subsequently a bilinear interpolation of the sound speed value was carried out.

In our second experiment, we used the sound speed, attenuation and density information to simulate signal raw data by a two-dimensional straight ray forward simulation. We simulated a hemispherical aperture with 64 emitters and 256 receivers (Figure 1b). The simulation is based on point scatterers at all positions where impedance changes occur. For discretization we calculate the impedance from the sound speed and density map and take the derivative to extract impedance changes at the interfaces of tissues. The scatter amplitude is proportional to the magnitude of the derivative. The time of flight and attenuation of reflections at these interfaces are calculated based on the sound speed and attenuation maps. Finally an optimal pulse[14] is folded into the signal for all time of flights of reflections and transmission. From the simulated signal raw data we reconstruct images using synthetic aperture focusing technique (SAFT) with sound speed and attenuation correction.[15] The purpose of the second experiment was two-fold: first, we analyzed whether the deformation field can be computed from SAFT images. Second, the reconstructed images are more realistic than ideal sound speed and attenuation images as they e.g. include typical imaging artifacts such as grating lobes.

2.4 Image-based strain estimation

After having set up a simulation framework based on biomechanical modeling and simulating USCT images in sections 2.2 and 2.3, the actual strain estimation method for USCT images needed to be developed. Several approaches have been proposed in literature for conventional ultrasound elastography. Most are operating on one-dimensional signal data acquired with and without compression and thereby consider axial deformation only.[16] Methods include e.g. the matching of signals by correlation.[8] Both axial and lateral displacement may be considered by two-dimensional estimators such as e.g. block matching.[17]

Due to the different imaging situation in USCT with transducers surrounding the object, signal based strain estimation cannot be trivially transferred from conventional ultrasound elastography. In this work we instead decided to estimate the two-dimensional displacement field based on the USCT images directly. This leads to a typical image registration problem in which the undeformed configuration of the breast is the reference image and the deformed configuration of the the breast is the moving image. As nonlinear deformations are expected in soft tissue, a nonlinear transformation model should be the method of choice.

In order to consider these requirements, our prototype implementation uses a non-rigid image registration based on a free-form deformation with cubic B-splines. For this purpose the MATLAB library "Medical Image Registration Toolbox" (MIRT) is used.[18] We selected a multi-resolution approach with five hierarchical levels.
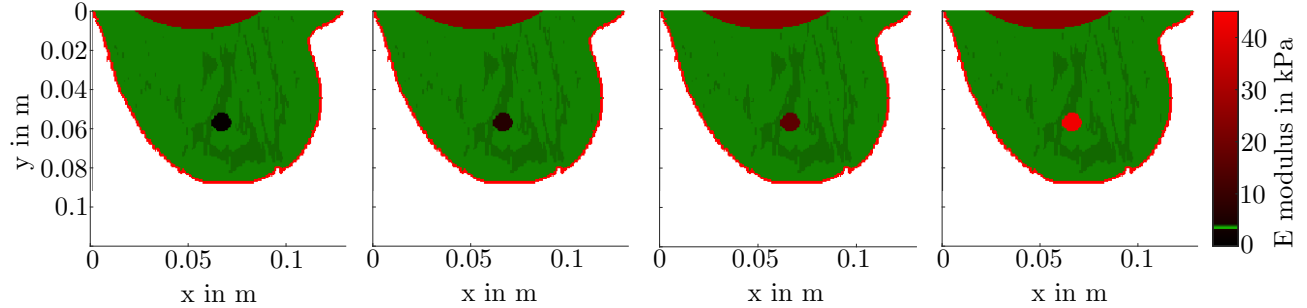
(a) Undeformed FEM model
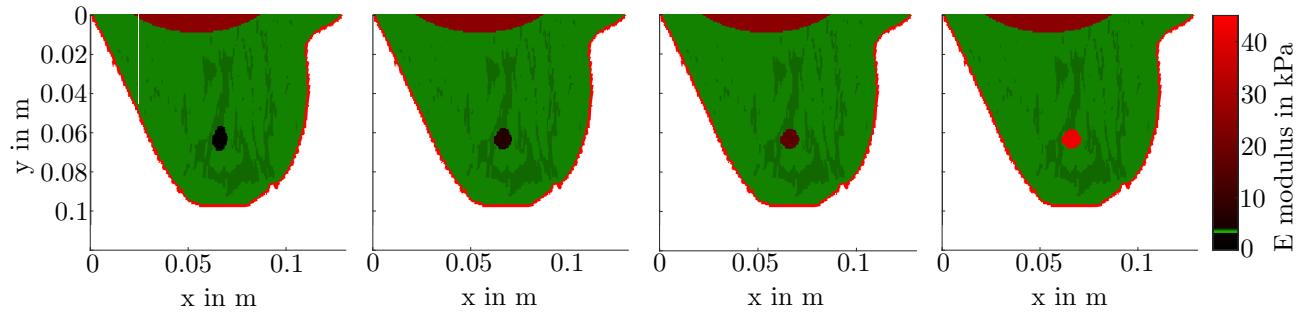
(b) Deformed FEM model

Figure 2: Polygon mesh of the breast model before (top) and after (bottom) the biomechanical simulation was applied. For the biomechanical simulation nodes close to the mamilla are pulled with a displacement of 10 mm. From left to right the E-modulus of the tumor was set to 1.00 kPa, 6.41 kPa, 16.38 kPa and 42.52 kPa.

The sum of squared differences (SSD) was used as similarity measure and the distance between the supporting points of the B-spline was set empirically to three pixels (1.5 mm) in order to allow complex deformations. The toolbox implements a gradient-based optimization (Implicit Euler method) and a curvature-based regularization (penalized Laplacian of the displacements). The maximum number of iterations at each hierarchical level was set to 500 and iterations were stopped if the similarity measure changes less than 10^{-5}.

Tissue specific stiffness reflects in more or less deformation relative to its surrounding tissue. Hence we are computing relative changes of the deformation field by visualizing the gradient magnitude of the deformation field for qualitative analysis.

For analysis in the second experiment we restrict the computation of the deformation field to a region of interest (ROI) around the lesion in order to stabilize the non-rigid image registration process.

3. RESULTS

Figure 2 shows the undeformed and deformed configuration of the breast phantom after performing the biomechanical simulation with different stiffness of the included tumor. From left to right material parameters for the neo-hookean material of the tumor were calculated from a Young's modulus (E-modulus) of 1.00 kPa, 6.41 kPa, 16.38 kPa and 42.52 kPa according to different tumor types measured in the ex-vivo experiments conducted by *Samani et al.*[11] For reference, the E-modulus of fatty and glandular tissue was 3.24 and 3.25 kPa respectively. Depending on its stiffness, the shape of the tumor is considerably different in the deformed configuration of the breast. With increasing E-modulus, the elongation of the lesion in y-direction reduces. In the extremest case (Figure 2b right), the lesion is barely deformed.

(a) $E_{Tumor} = 1.00\,\text{kPa}$

(b) $E_{Tumor} = 6.41\,\text{kPa}$

(c) $E_{Tumor} = 16.38\,\text{kPa}$

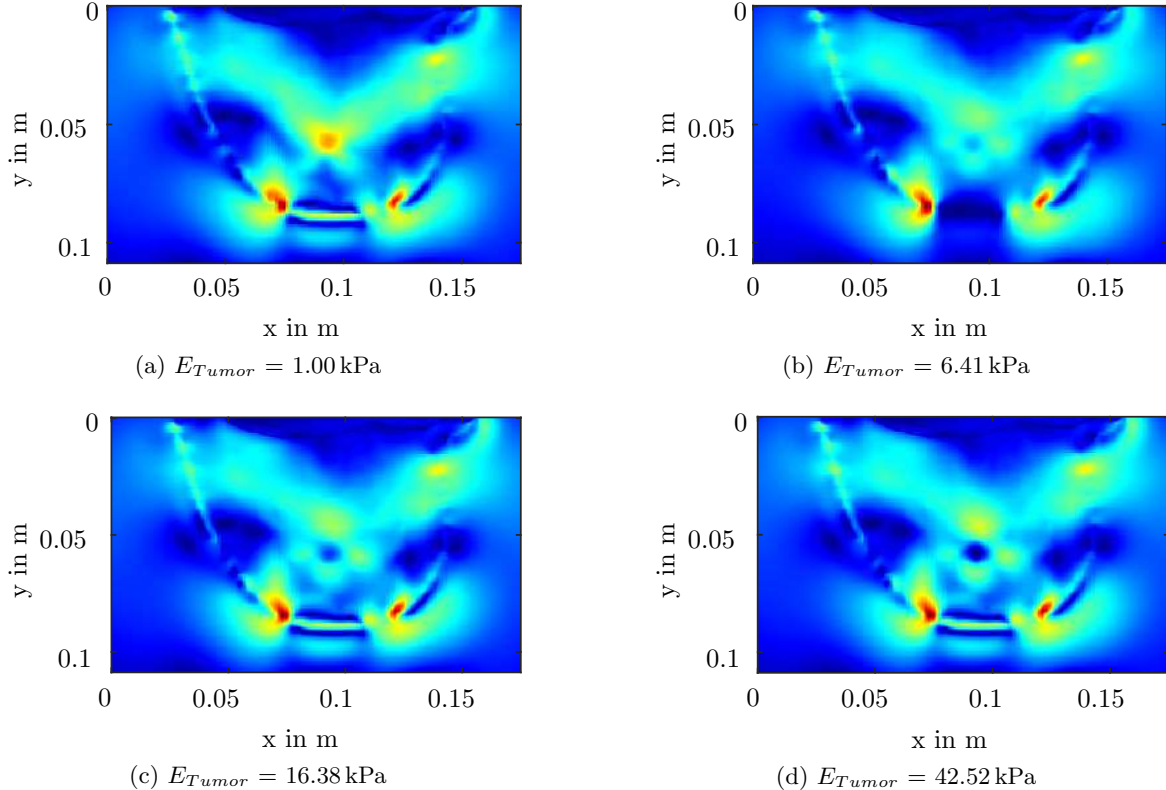(d) $E_{Tumor} = 42.52\,\text{kPa}$

Figure 3: Magnitude of the gradient of the deformation field estimated by non-rigidly registering the deformed to the undeformed sound speed image. The value range has been normalized to the maximum magnitude of all cases. The colormap ranges from blue (low values) to red (high values).

For our first experiment we used the ideal sound speed image for estimation of the deformation field as described in section 2. We display the gradient of the magnitude of the deformation field for the entire breast in figure 3. For the lesion which is less stiff than the surrounding tissue (Figure 3a, ratio of E-modulus between lesion and surrounding tissue approximately 0.3), a high gradient magnitude can be observed at the position of the lesion (red color), while for all lesions which are modeled stiffer than the surrounding tissue (Figures 3b to 3d, ratios equaling 2.0, 5.1 and 13.1 respectively), the gradient magnitude is comparably low (dark blue color). Especially close to the front of the breast, where displacement nodes were defined for the deformation simulation, artifacts can be observed as the non-rigid registration seems to compensate small deformations between rigidly and non-rigidly deformed areas: for nodes subject to the boundary condition of the FEM simulation, the displacement is constant, while nearby nodes may be displaced strongly due to the applied force. Furthermore a low-frequent displacement artifact with medium magnitude can be observed extending from the tumor position towards the breast surface (light blue color). Nevertheless the tumor can in all cases be visually differentiated from surrounding tissue.

For the second experiment, we estimated the deformation field from the reconstructed SAFT images in a ROI, assuming that the suspicious lesion is depicted in the SAFT image and that the ROI can be defined by an operator as in conventional elastography. Figure 4 illustrates the result of the image registration process of this ROI for the case in which the lesion had a lower stiffness as the surrounding tissue. The undeformed image (Figure 4, first image) was used as reference image and the deformed image (Figure 4, second image) was used as moving image. After applying the non-rigid registration, the structures in the deformed image line up well with the undeformed image as illustrated in the third and fourth image of Figure 4.

From the deformation field which was computed to derive the registered deformed image, the gradient was calculated as presented in section 2.4. Figure 5 shows the normalized magnitude of the gradient of the deformation
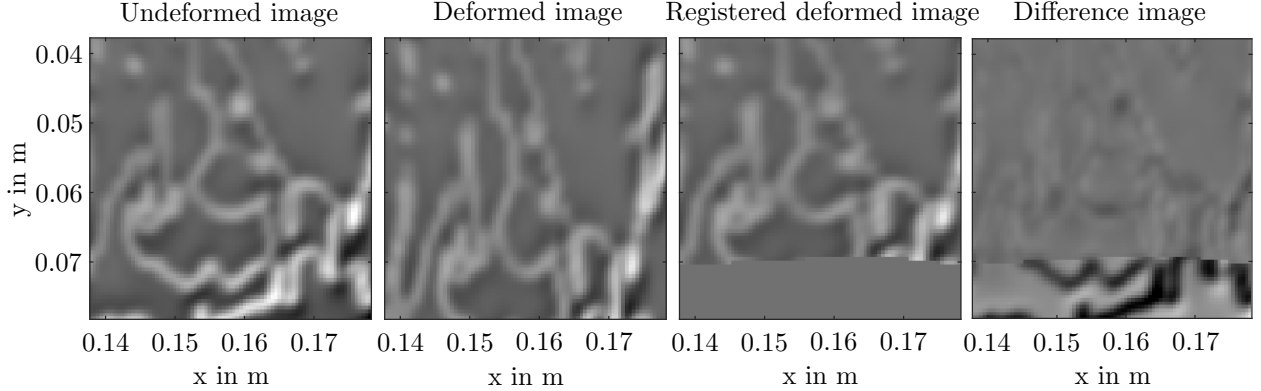
Figure 4: Illustration of the image registration process between undeformed SAFT image and deformed SAFT image. After applying the non-rigid registration the registered deformed image is derived. As can be seen in the difference image between the registered deformed image and the undeformed image, the structures line up well. This example shows the case in which the tumor has an E-modulus of 1 kPa.

field as a semi-transparent colored overlay on the reconstructed SAFT image. The same colormap as in the first experiment has been used ranging from dark blue (low values) to red (high values). For the low stiffness lesion (Figure 5a) a high gradient magnitude can be observed (red color) at the position of the tumor as it is highly deformed compared to surrounding tissue. For stiffer lesions (Figures 5b to 5d), the gradient magnitude is considerably smaller inside the tumor (blue/turquoise color) as the tumor does change its shape only marginally by the breast deformation. A halo of higher magnitude can be observed around the lesion, which expresses the increased deformation of surrounding tissue. The representation of the stiffness analysis is gradually changing from low to high stiffness.

4. DISCUSSION AND CONCLUSION

In this work we presented a novel approach, called USCT-SE, to perform strain elastography imaging with ultrasound computer tomography setups. To our knowledge this is the first time such an approach has been proposed. The aim of this paper was to verify the feasibility using simulated data. For this purpose we applied a non-linear biomechanical model to obtain realistic image data of a deformed and undeformed breast. For strain analysis we applied a non-rigid image registration between the deformed and undeformed breast to derive the deformation field. The magnitude of the gradient is used for visual representation of relative tissue stiffness. Results of the strain analysis show that soft and hard lesions can be distinguished visually in the elastograms. Also a trend can be observed, that by the color scale the tumors of different stiffness higher than the surrounding tissue can be distinguished relative to each other.

Until now the strain analysis has been limited to ideal sound speed images and slightly more realistic simulated SAFT images. In future the method needs to be validated with more realistic noisy data, data containing artifacts and finally also with experimental data. A simple image-based analysis with a non-rigid registration has been applied to obtain the deformation field. While this method was able to distinguish soft and hard lesions visually in nearly ideal data, artifacts in the images can be observed, especially close to the displacement device. This can potentially be mitigated by a different regularization or locally adaptive spacing of the supporting points of the B-Spline deformation. For experimental data, the application of this method needs to tested and optimized as artifacts in the reconstructed images may cause the optimization of the non-rigid registration to be stuck in local minima.

This paper provides a very first approach to obtain mechanical information based on external mechanical excitation of breast tissue in a USCT system. In existing 2D respectively 2.5D systems,[1,2] in which a displacement device can easily be mounted outside the transducer plane, the mechanical excitation may already be achieved without major loss in image quality. Further research would be required with respect to the optimization of the displacement magnitude, which until now was set empirically to 10 mm in the biomechanical simulation.

(a) $E_{Tumor} = 1.00\,\text{kPa}$

(b) $E_{Tumor} = 6.41\,\text{kPa}$

(c) $E_{Tumor} = 16.38\,\text{kPa}$

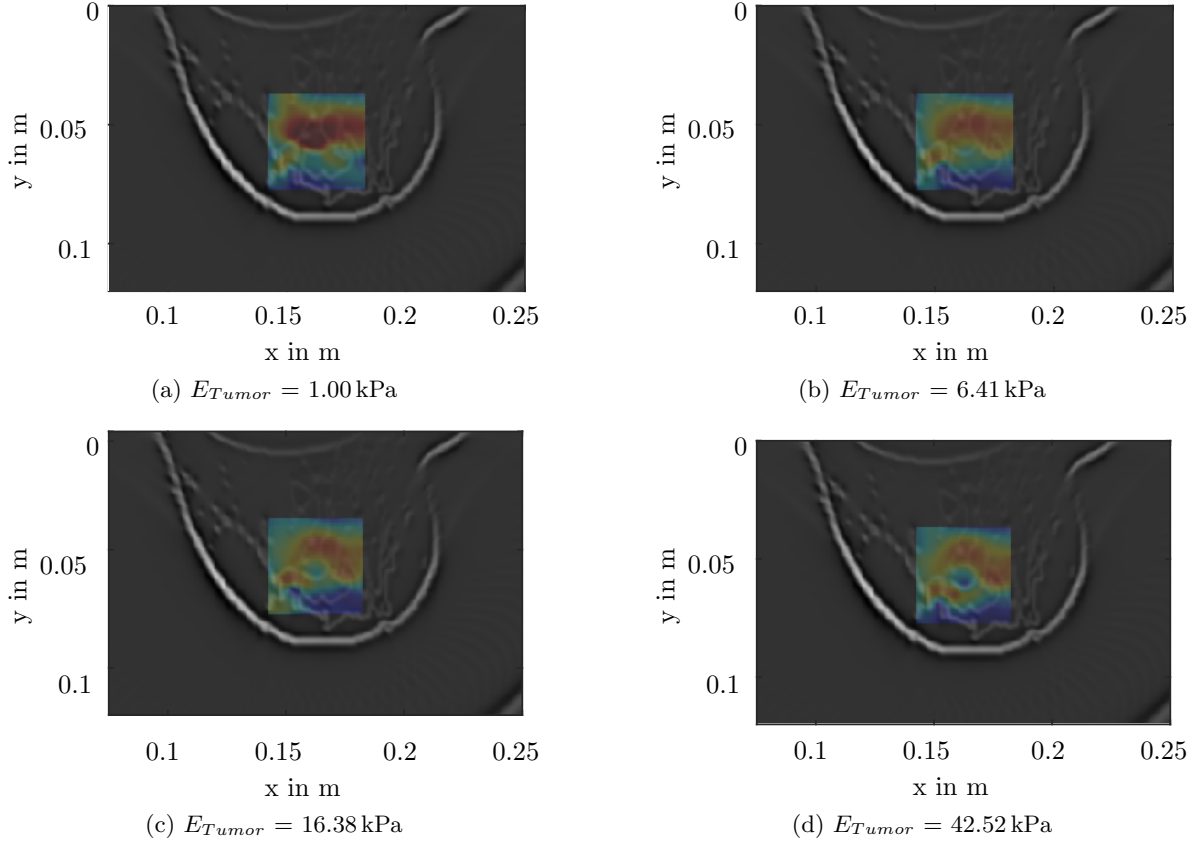(d) $E_{Tumor} = 42.52\,\text{kPa}$

Figure 5: Gradient of the magnitude of the deformation field semi-transparently overlaid on the reconstructed SAFT images. The deformation has been estimated in the colored ROI by non-rigidly registering the deformed to the undeformed cutout from the reconstructed SAFT image. The colormap ranges from blue (low values) to red (high values).

Furthermore the influence of the limited out-of-plane resolution of 2D and 2.5D systems will need to be analyzed since the mechanical excitation – and thereby the most prominent deformation of the breast – is applied out-of-plane. Finally, the image-based strain analysis will need to be extended to 3D for analysis of volumetric images. 3D USCT systems[3] may on the one hand solve possible problems of the limited out-of-plane resolution. On the other hand, mounting of a displacement device will be more complex since it would need to be positioned inside the transducer half-sphere, which may cause additional artifacts in the images.

In future the mechanical excitation may be extended to e.g. inducing vibrations from a vibration plate close to the patient's breast or internal displacement of tissue by acoustic radiation force using a focusing of transducers. The latter two methods would allow implementing shear-wave elastography to quantify the Young's modulus of tissues if sufficient frame rates can be achieved.

To conclude, the simulation methods presented in this paper may serve as a basis to analyze the feasibility of elastography approaches with USCT. The results obtained for the exemplary USCT-SE implementation are promising and may potentially be applied to existing systems without major modification.

REFERENCES

[1] Duric, N., Littrup, P., Roy, O., Li, C., Schmidt, S., Cheng, X., and Janer, R., "Clinical breast imaging with ultrasound tomography: A description of the SoftVue system," *The Journal of the Acoustical Society of America* **135**(4), 2155–2155 (2014).

[2] Wiskin, J. W., Borup, D. T., Iuanow, E., Klock, J., and Lenox, M. W., "3-D Nonlinear Acoustic Inverse Scattering: Algorithm and Quantitative Results," *IEEE Transactions on Ultrasonics, Ferroelectrics, and Frequency Control* **64**(8), 1161–1174 (2017).

[3] Gemmeke, H., Hopp, T., Zapf, M., Kaiser, C., and Ruiter, N. V., "3D ultrasound computer tomography: Hardware setup, reconstruction methods and first clinical results," *Nuclear Instruments and Methods in Physics Research Section A: Accelerators, Spectrometers, Detectors and Associated Equipment* **873**, 59–65 (2017).

[4] Krouskop, T. A., Wheeler, T. M., Kallel, F., Garra, B. S., and Hall, T., "Elastic Moduli of Breast and Prostate Tissues under Compression," *Ultrasonic Imaging* **20**(4), 260–274 (1998).

[5] Garra, B. S., Cespedes, E. I., Ophir, J., Spratt, S. R., Zuurbier, R. A., Magnant, C. M., and Pennanen, M. F., "Elastography of breast lesions: initial clinical results.," *Radiology* **202**(1), 79–86 (1997).

[6] Duric, N., Peter Littrup, M. D., Li, C., Roy, O., Schmidt, S., Seamans, J., Wallen, A., and Bey-Knight, L., "Whole breast tissue characterization with ultrasound tomography," in [*Proceedings Medical Imaging 2015: Ultrasonic Imaging and Tomography*], **9419**, 81–88, SPIE (2015).

[7] Gennisson, J.-L., Deffieux, T., Fink, M., and Tanter, M., "Ultrasound elastography: Principles and techniques," *Diagnostic and Interventional Imaging* **94**(5), 487–495 (2013).

[8] Ophir, J., Céspedes, I., Ponnekanti, H., Yazdi, Y., and Li, X., "Elastography: A quantitative method for imaging the elasticity of biological tissues," *Ultrasonic Imaging* **13**(2), 111–134 (1991).

[9] Hopp, T., Dietzel, M., Baltzer, P. A., Kreisel, P., Kaiser, W. A., Gemmeke, H., and Ruiter, N. V., "Automatic multimodal 2D/3D breast image registration using biomechanical FEM models and intensity-based optimization," *Medical Image Analysis* **17**(2), 209–218 (2013).

[10] Smole, P. C., Kaiser, C., Krammer, J., Ruiter, N. V., and Hopp, T., "A Comparison of Biomechanical Models for MRI to Digital Breast Tomosynthesis 3D Registration," in [*Computational Biomechanics for Medicine*], Nielsen, P. M. F., Wittek, A., Miller, K., Doyle, B., Joldes, G. R., and Nash, M. P., eds., 107–117, Springer International Publishing (2019).

[11] Samani, A., Zubovits, J., and Plewes, D., "lastic moduli of normal and pathological human breast tissues: an inversion-technique-based investigation of 169 samples," *Physics in medicine and biology* **52**(6), 1565–1576 (2007).

[12] Gefen, A. and Dilmoney, B., "Mechanics of the Normal Woman's Breast," *Technol. Health Care* **15**(4), 259–271 (2007).

[13] Hasgall, P. A., Di Gennaro, F., Baumgartner, C., Neufeld, E., Lloyd, B., Gosselin, M. C., Payne, D., Klingenböck, A., and Kuster, N., "IT'IS Database for thermal and electromagnetic parameters of biological tissue, Version 4.0." Website: itis.swiss/database (2018).

[14] Ruiter, N. V., Schwarzenberg, G. F., Zapf, M., and Gemmeke, H., "Improvement of 3D ultrasound computer tomography images by signal pre-processing," in [*Proceedings 2008 IEEE Ultrasonics Symposium*], (2008).

[15] Kretzek, E., Hopp, T., and Ruiter, N. V., "GPU-based 3D SAFT reconstruction including attenuation correction," in [*Proceedings Medical Imaging 2015: Ultrasonic Imaging and Tomography*], **9419**, 66–74, SPIE (2015).

[16] Sigrist, R. M. S., Liau, J., Kaffas, A. E., Chammas, M. C., and Willmann, J. K., "Ultrasound Elastography: Review of Techniques and Clinical Applications," *Theranostics* **7**(5), 1303–1329 (2017).

[17] Zhu, Y. and Hall, T. J., "A Modified Block Matching Method for Real-Time Freehand Strain Imaging," *Ultrasonic Imaging* **24**(3), 161–176 (2002).

[18] Myronenko, A., *Non-rigid Image Registration: Regularization, Algorithms and Applications*, PhD thesis, Oregon Health and Science University (2010).